Aerosol and Air Quality Research

ORIGINAL RESEARCH
https://doi.org/10.4209/aaqr.200624

Chemical Fingerprints for $PM_{2.5}$ in the Ambient Air near a Raw Material Storage Site for Iron Ore, Coal, Limestone, and Sinter

Kavita Justus Mutuku[1], Yen-Yi Lee[2,3*], Guo-Ping Chang-Chien[2,3], Sheng-Lun Lin[4], Wei-Hsin Chen[5,6,7*], Wen-Che Hou[1]

[1] Department of Environmental Engineering, National Cheng Kung University, Tainan 70101, Taiwan
[2] Super micro mass research and technology center, Cheng Shiu University, Kaohsiung 833, Taiwan
[3] Center for Environmental Toxin and Emerging-Contaminant Research, Cheng Shiu University, Kaohsiung 833, Taiwan
[4] School of Mechanical Engineering, Beijing Institute of Technology, Beijing 100081, China
[5] Department of Aeronautics and Astronautics, National Cheng Kung University, Tainan 70101, Taiwan
[6] Research Center for Smart Sustainable Circular Economy, Tunghai University, Taichung 407, Taiwan
[7] Department of Mechanical Engineering, National Chin-Yi University of Technology, Taichung 411, Taiwan

ABSTRACT

To understand the contributions of a raw material storage site for iron ore, coal, limestone, and sinter to ambient air fine particulate matter ($PM_{2.5}$), the concentrations and chemical fingerprints for resuspended and ambient air $PM_{2.5}$ were compared. Investigations were done for 15 piles of raw materials, including 5 iron piles, 5 coal piles, 3 stone piles, and a single pile each for coke and sinter. Additionally, four sites, including A, B, C, and D, in the storage site surroundings were chosen to investigate the ambient air $PM_{2.5}$ concentrations. The concentrations, compositions, and i and j values for $PM_{2.5}$ varied significantly by season in the four sites under investigation. The chemical fingerprints of the $PM_{2.5}$ showed that water-soluble ions were the most important component in all sites. Specifically, SO_4^{2-} and NO_3^- were the predominant water-soluble ions in winter and summer, respectively. The most dominant components in the iron ore, coal, limestone, coke, and sinter piles were iron, carbon, Ca^{2+} and carbon, carbon and SO_4^{2-}, and Fe and Ca^{2+}, respectively. During the summer, $PM_{2.5}$ concentrations ranged from 13.7–18.0 μg m^{-3}, where the chemical composition of water-soluble ions, metals, carbon accounted for 54.2%, 5.7%, and 23.7% respectively. During winter, the concentrations ranged from 44.7–48.0 μg m^{-3}, where the water-soluble ions, metals, carbon components accounted for 49.2%, 8.1%, and 17.4% respectively. From the chemical mass balance, the main sources of $PM_{2.5}$ in sites B, C, and D were stationary sources, mobile sources, and secondary organic aerosols. To effectively address the air pollution threat associated with the surroundings of a raw material storage site, the environmental protection agency should formulate measures to effectively reduce the contribution of resuspended dust and other pollution sources to ambient air $PM_{2.5}$.

Keywords: $PM_{2.5}$, Chemical fingerprints, Raw materials, Re-suspension, Seasonal variation

OPEN ACCESS

Received: November 10, 2020
Revised: December 27, 2020
Accepted: December 27, 2020

* **Corresponding Authors:**
Yen-Yi Lee
leeyenyi@gcloud.csu.edu.tw
Wei-Hsin Chen
chenwh@mail.ncku.edu.tw;
weihsinchen@gmail.com

Publisher:
Taiwan Association for Aerosol Research
ISSN: 1680-8584 print
ISSN: 2071-1409 online

1 INTRODUCTION

Deteriorating air quality caused by elevated concentrations of fine particulate matter ($PM_{2.5}$)

from a raw material storage site for iron ore, coal, limestone, and sinter is a great cause of concern to the residents in the southern region of Taiwan. In the steel production industry, $PM_{2.5}$ is emitted during manufacturing as well as during the resuspension process at raw material storage sites. The iron ore sintering process for steel plants requires several materials, including iron ore, coal, limestone, coke, and recycled steel (Fernández-González *et al.*, 2017). Contingent on the particle size distribution and chemical compositions, the concentrations of $PM_{2.5}$ differ among piles of raw materials. Recently, existing plants have expanded their production due to increased demand for steel (Cullen *et al.*, 2012). Consequently, information published by the Taiwan Emission database system (TEDS 9.0) shows that the steel industry is responsible for 15.9% of the total $PM_{2.5}$ emitted nationwide.

There are both natural and anthropogenic sources of $PM_{2.5}$. However, emissions from the latter are believed to impact human health more adversely (Artíñano *et al.*, 2003; Weijers *et al.*, 2011). Major anthropogenic sources of fine particulates are associated with modern industrialization activities such as combustion, construction, manufacturing processes, and road dust (de la Campa *et al.*, 2010; Benchrif *et al.*, 2018). A comparison study between the pollution contributions from long-range transportation from neighboring China and those from local sources in cities within Taiwan established that the later was more dominant (Lai and Brimblecombe, 2021).

Previous analyses of $PM_{2.5}$ in Taiwan indicate several components, including, organic and elemental carbon, metals, crust elements, and water-soluble ions (Wang *et al.*, 2020). Metallic components in $PM_{2.5}$ from industrial processes are not easily removed by pollution control devices. Consequently, they end up being discharged into the atmosphere (Ahmad *et al.*, 2018). Recent surveys on the concentrations of metal components in particulate matter from six air quality monitoring stations including Nanzi, Zuoying, Sanmin, Qianjing, Qianzheng, and Xiaogang found significant concentrations of Al, Ca, Fe, and K. Overall, Fe was the most abundant metal, and Xiaogang station had the highest concentration (Lin *et al.*, 2008; She *et al.*, 2020).

Research on $PM_{2.5}$ is mostly focused on four processes: emission, transformation, transportation, and deposition (Pöschl, 2005; Choi *et al.*, 2007; Shen *et al.*, 2020). The latter is critical to the human population since it directly impacts their health. Deposition can be divided into wet and dry deposition. In wet deposition, the constituents of $PM_{2.5}$ are washed by precipitation culminating on solid surfaces such as land and vegetation or in water masses such as lakes, rivers, and oceans (Zhao *et al.*, 2018). Through dry deposition, fine particulates wind up on surfaces or in human or animal lungs during inhalation (Zhang *et al.*, 2014). Researchers have established reliable methods for sample collection and quantification of particulate matter. Loo *et al.* (1975) describe the application of a dichotomous sampler to collect both fine and coarse particulate matter. Receptor models for connecting the ambient air $PM_{2.5}$ and their emission sources have been developed and applied in many studies (Houck, 1991; Pace, 1991; Wienke *et al.*, 1994).

Inhalation of $PM_{2.5}$ has been linked to several adverse health effects on the respiratory system including inflammation, cancer, and exacerbation of pre-existing respiratory conditions (Chalupa *et al.*, 2004; Feng *et al.*, 2016). Additional adverse health effects to the rest of the human body include the destruction of the nervous and circulatory systems, aggravation of diabetes mellitus, and anomalies in newborns (Nogueira, 2009; Zhao *et al.*, 2013). Several $PM_{2.5}$ components including, Ca, black carbon, V, and Zn are associated with cardiovascular hospitalization while road dust, sea salt, aluminium, calcium, chlorine, black carbon, nickel, silicon, titanium, and vanadium are linked to respiratory complications (Bell *et al.*, 2014). According to a study by Dejmek *et al.*, (1999), the odds ratio for intrauterine growth retardation upon exposure of pregnant mothers to $PM_{2.5}$ is 1.26. Additionally, women with high pre-pregnancy exposure to $PM_{2.5}$ experience increased incidences of gestational diabetes mellitus (Monshi and Asgarani, 1999).

In the study of emission sources of particulates, resuspension, which is the removal of initially deposited material through a mechanical process such as wind, traffic, and soil cultivation, is rarely covered. Resuspended $PM_{2.5}$ can be transported to residential areas and rise to levels coinciding with the average breathing zone hence posing an inhalation exposure risk to residents. Herein, the chemical fingerprints of resuspended $PM_{2.5}$ from a raw material storage site and its contribution to ambient $PM_{2.5}$ in the surrounding area were investigated. A receptor model called chemical mass balance (CMB) was applied to estimate the contribution of different pollution sources to ambient $PM_{2.5}$. To the authors' knowledge, a study on the contribution of resuspended particles from a raw material storage site to ambient air $PM_{2.5}$ has not been carried out before.

Therefore, this study can fill this research gap and provide useful insights into developing pollution control strategies for affected emission sources. Gathering comprehensive knowledge of emission sources and the chemical composition of $PM_{2.5}$ in the surroundings of the storage site is an appropriate step towards understanding the overall air quality to create proper health guidelines for the residents in the neighborhood.

2 METHODOLOGY

2.1 Sample Collection at the Raw Material Storage Field and its Surroundings

The area under investigation was separated into four sites, herein referred to as sites A, B, C, and D, as shown in Fig. 1. Site A encompasses the raw material storage zone. Sites B and C are densely populated areas next to the raw material storage site. Site D is also densely populated but further from the raw material storage site compared to sites B and C. Samples were collected at the raw material storage site for three days in each season to represent summer and winter. The sampling dates for the two seasons were the 5th, 8th, and 11th of August for summer and the 9th, 15th, and 27th of December for winter. Sampling dates were synchronized with the dates of $PM_{2.5}$ manual inspections for the EPA monitoring station. Additionally, a peripheral airborne particulate sampler (BGI PQ200) was applied to collect samples continuously for 24 hours.

A total of 15 samples were collected to represent each of the following: 5 piles of irons ore (iron ore 1–5), 5 piles of coal (coal pile 1–5), 3 piles of limestones (limestone 1–3), 1 pile each of sinter and coke. Special care was taken to adhere to the soil sampling method (S102.63B) announced by the National Institute of Environmental Analysis (NIEA). The topsoil samples were divided into composites and grab samples. Samples from different sampling points on the horizontal surface were mixed to obtain the average concentration for that specific area. A virtual grid was applied to collect the samples at the intersections as well as within the grids.

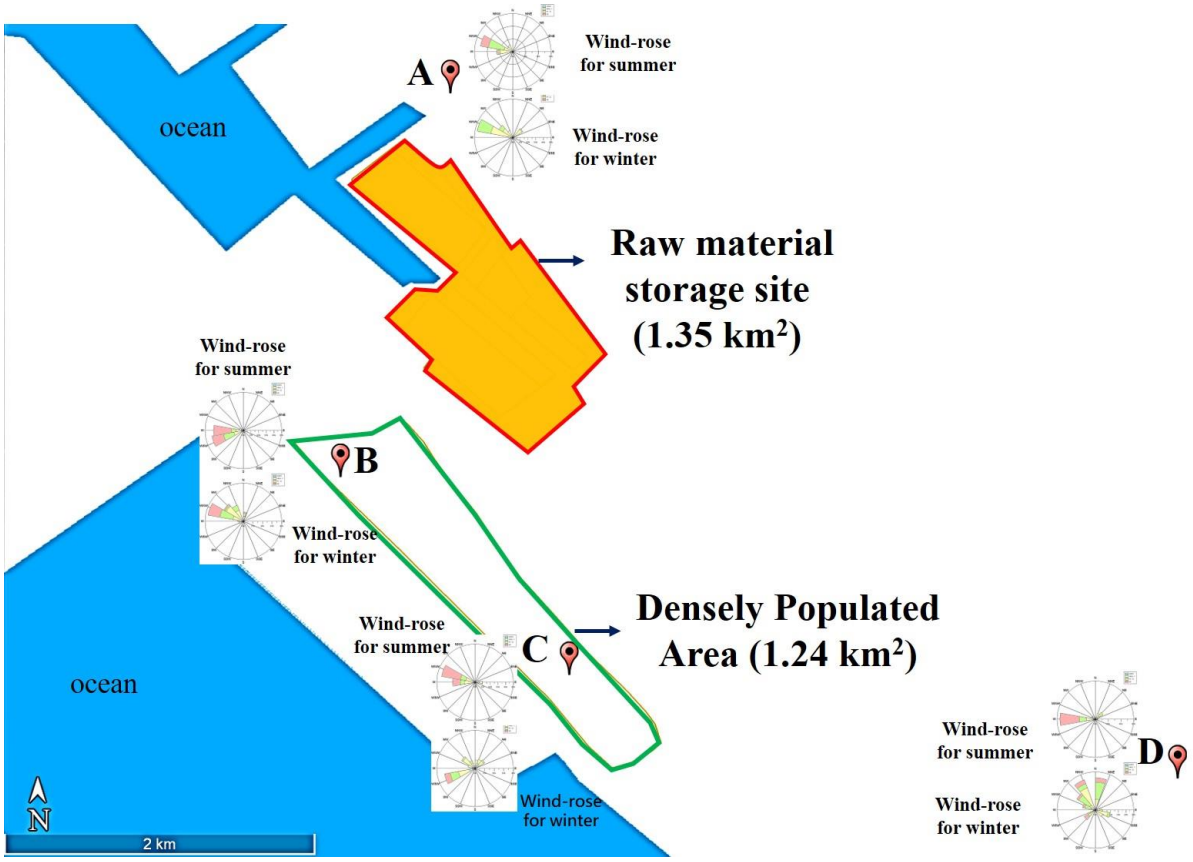

Fig. 1. A plan view of the raw material storage site in the area under investigations and the distribution of the sampling points for ambient air $PM_{2.5}$ including A, B, C, and D.

The soil samples were obtained and put in separate plastic lock bags. Reagents used for the treatment of the soil samples included phosphate-free detergent, distilled water, acetone, and n-hexane. Decontamination of the sampling equipment was performed between the collection of consecutive samples. A metal brush was used to remove debris from the equipment; a non-phosphorus detergent was applied on a brush, after which the device was brushed thoroughly before rinsing with distilled water and then with organic solvents (acetone or n-ethane). Lastly, the sampling device was rinsed with distilled water.

2.2 Re-suspension Tests

After obtaining the coarse and fine particulate matters from the sample (PM_{10} and $PM_{2.5}$) a resuspension test was performed. The resuspension chamber was carefully constructed and set to accurately represent natural wind. A resuspension system was used to administer tests to determine both the vertical and lateral translocation of fine particulates within an enclosed space. The re-suspension test was performed for the portion of the total suspended solids (TSP) that passed through a 400-mesh screen ($D < 38$ μm) and reached the bottom plate. The powder was collected in a stainless-steel dish and then loaded into a dry powder generator. An accelerated airflow rate of 16.7 L min^{-1} was applied to simulate natural wind in the 1 m square horizontal cross-section and 2 m high re-suspension chamber. A dichotomous sampler for PM_{10} and $PM_{2.5}$ was used to collect coarse and fine particulate matter. A dichotomous sampler was placed under the re-suspension chamber**.** The total time for re-suspension and sample collection was 5 minutes.

2.3 Weighing and Conditioning of the Samples

A microbalance was used for the 24 filter paper samples. The inspection was done for each sampling filter paper using a lamp and a magnifying glass to confirm the integrity of the filter paper. The following factors were considered to compromise the integrity of the filter paper: breakage, indentations, dents, scratches, fiber, and particle contamination. Care was taken to preserve the integrity of the filter paper during unpackaging, weighing, conditioning, and clipping. The filter paper was then placed in a conditioning environment for 12 hours. This was succeeded by fine weighing. The steps for the conditioning and fine weighing were repeated until the difference in weight was constant and less than 5 μg. The average of the weight before and after conditioning was taken as the weight after sampling. The formula for the calculation of $PM_{2.5}$ concentration is as follows:

$$PM_{2.5}\ \text{Concentration} = \frac{W_f - W_i}{V_a} \tag{1}$$

where $PM_{2.5}$ concentration is in μg m^{-3}. W_i and W_f represent the masses of the filter paper in μg before and after sampling, respectively. V_a is the total volume of air in m^3.

To collect samples for ambient air $PM_{2.5}$, blank filter papers were exposed to the atmosphere for 24 hours with a sample volume of 24 m^3. The detection limit was 2 μg m^{-3}.

2.4 Analysis of Metal Compositions, Water-soluble Ion Components, and Carbon Content

Evaluating the chemical fingerprints for $PM_{2.5}$, involved establishing their metal components, water-soluble ion concentrations, and carbon content. A total of 15 samples were tested for 31 metal elements including Li, Be, Na, Mg, Al, K, Ca, Ti, V, Cr, Mn, Fe, Co, Cu, Zn, Ga, As, Se, Rb, Sr, Ag, Cd, In, Sn, Cs, Ba, Tl, Pb, U, Ni, and Si. Further analyses were done for 4 anionic species including SO_4^{2-}, NO^-, Cl^-, F^-, and 5 cationic species including Na^+, K^+, Ca^{2+}, Mg^{2+}, NH_4^+. The concentrations of elemental and organic carbons (EC and OC) were evaluated.

The metal composition analyses for $PM_{2.5}$ were performed using the other half of the Teflon filter paper. The microwave digestion pretreatment process established by the Environmental Protection Administration (EPA) was applied. First, calibration was done using five standard solutions to produce a calibration line. The relative error value of the calibration line was set to be within ±10%. Otherwise, the operating condition of the instrument must be checked or

maintenance must be performed and another calibration line must be developed. After calibration, the samples were put into ICP/MS for analysis. The blank sample could not exceed double the MDL. A blank sample was prepared and analyzed after every 10 samples. Care was taken to ensure a recovery rate of 80–120%. Furthermore, one sample was tested twice in every batch of 10 samples. The relative difference between the two measurements could not exceed 20%. Quantification of the metal composition in the $PM_{2.5}$ samples was performed using high-resolution inductively coupled plasma mass spectrometry (ICP-MS, Agilent 7500A). The calibration line was checked using a standard solution whereby the acceptable absolute error was required to be less than 10%.

Sample pretreatment involved shaking half of each collected Teflon filter using ultrasonic vibrations for 90 minutes in 10 mL of deionized water. After extraction, the 10 mL was poured into a syringe and filtered with a 0.45 μm membrane to remove particles. Quantification of the water-soluble anions was performed using an Ion Chromatograph (IC) (Dionex, Model DX-120) series conductivity detector. Analysis of the anions was performed with the ASRS-ULTRA suppressor, Ion Pac AS4A-SC column, and Na_2CO_3/$NaHCO_3$ eluent. In addition, cations were evaluated using a CSRS-ULTRA suppressor, an Ion Pac CS12 column, and 0.1 M of H_2SO_4 eluent. The concentrations in the blank samples fell below the limit of detection (LOD) for all ions. Therefore, deductions were unnecessary for the calibration data.

An elemental analyzer (Elementar Vario MIRCO Cube), with the AS 200 type Autosampler and DP 700 integrator for were used to quantify both the EC and OC. The equipment's precision and stability are shown in Table 1**,** and its operating conditions are provided in Table 2. A quartz filter paper was first placed in the thermal chamber and heated to 900°C to remove any available carbon before the chemical analysis. Analysis of the carbon content in $PM_{2.5}$ involved instantaneous dynamic oxidation. The sample's chemical bonds were broken in the quartz reaction tube. It was rapidly oxidized to CO_2, after which it was reduced using Cu and then passed through the separation column for detection using a thermal conductivity detector (TCD). The organic carbon content was obtained based on the difference between the total carbon (TC) and EC.

2.5 Chemical Mass Balance

A chemical mass balance was applied for the nearby emission sources, including the raw material storage site, background soil dust, traffic dust, mobile sources, steel industry, various industrial boilers, electric arc furnaces, coke ovens, sintering furnaces, power plants, and incinerators, as shown in Table 1. Criteria for the selection of emission sources included a chi-square value of less than 4.0, press normalization $R^2 > 0.8$, a t-statistic > 2.0, where the ratio of the calculated to the measured value was required to be 0.8–1.2, the residual and uncertainty ratio was required to be –2.0–2.0, and unquantified and similar clusters should preferably be absent.

The theory of the receptor model was based on the similarities between the chemical compositions of emission sources and those of the receptor sites. It was supported by the principle of conservation of mass and statistics. The pollutant concentration at the receptor point was the linear summation of the pollution sources. The main simplifying assumption is that

Table 1. Precision and stability of element analyzer.

Carrier gas	Accuracy	Precision
Helium	≤ 0.3%	≤ 0.2%
Argon	≤ 0.5%	≤ 0.4%

Table 2. Operating conditions of element analyzer.

Process	Set conditions
Oxidation furnace temperature (°C)	1020
Reduction furnace temperature (°C)	500
Carrier gas flow rate (mL min^{-1})	100
Sample delay time (s)	8–15
Total execution time (min)	9–12

there were no chemical reactions between different chemical species from the emission sources. A fingerprint database required for the chemical mass balance receptor model was established before the CMB8.2 receptor model was applied to estimate the respective percentage contributions of the $PM_{2.5}$ sources to ambient air $PM_{2.5}$.

3 RESULTS AND DISCUSSION

3.1 Ambient Air $PM_{2.5}$ Concentration during Summer and Winter

Kaohsiung has a tropical climate, where rainfall is experienced 5–9 months of the year. The average annual temperature is approximately 24.3°C while the annual rainfall is approximately 1738 mm (Chen and Chen, 2003). During summer, warm, and humid air masses flow from the southern side of the country, which is mostly ocean. Under rainfall and typhoon conditions, the relative humidity ranges between 69.85 and 74.76%. Wind flow over the Kaohsiung region leads to lower relative humidity in winter, which ranges between 67.51 and 70.60%.

From 2005 to 2017, the EPA compared manually calculated hourly concentrations for $PM_{2.5}$ to those from an automatic monitoring station. The $PM_{2.5}$ annual average concentration for 13 years is presented in Fig. 2. There has been a steady decrease in the concentration of $PM_{2.5}$ in Xiaogang

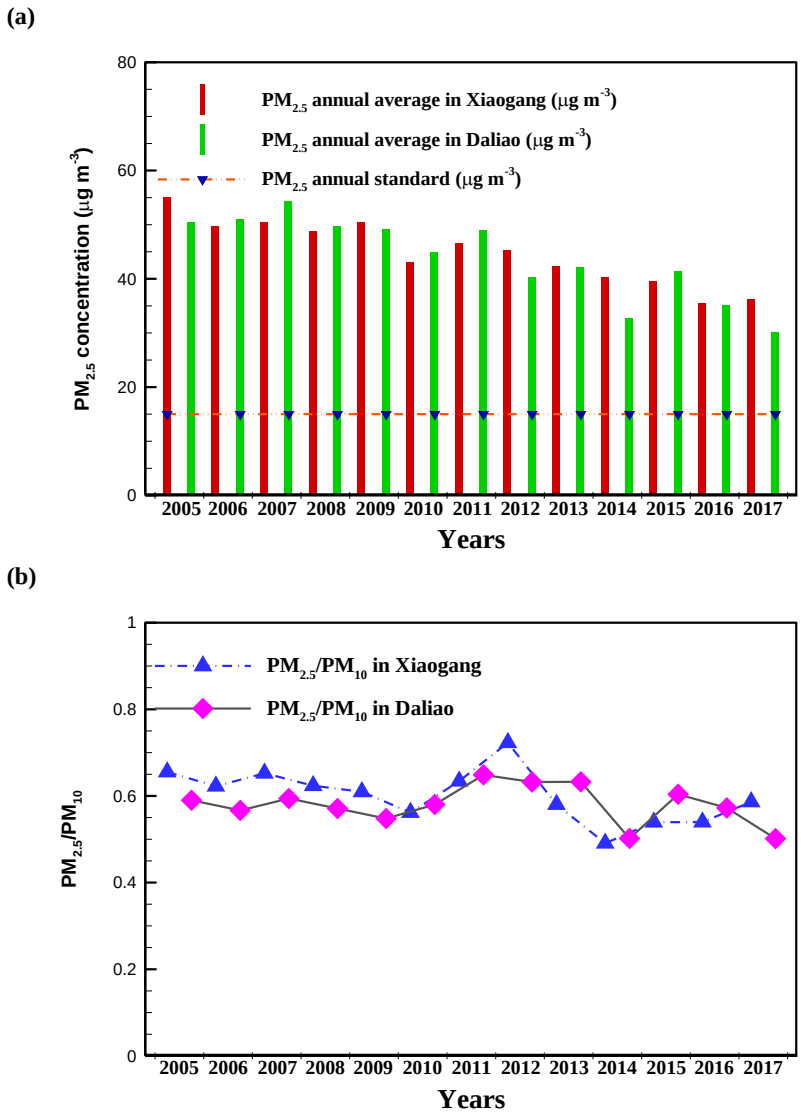

Fig. 2. Annual values for (a) ambient air $PM_{2.5}$ concentrations and (b) $PM_{2.5}$ to PM_{10} ratios in Daliao and Xiaogang stations for the years 2005 to 2017.

station from 55.2 μg m^{-3} in 2005 to 36.2 μg m^{-3} in 2017. Similarly, in Daliao, the concentrations were 50.4 and 3.02 μg m^{-3} in the respective years. The reduction over the period was 34.4% and 40.1% for Xiaogang and Daliao stations, respectively. The Taiwan EPA has put control measures to reduce the emission for air pollutants including $PM_{2.5}$, PM_{10}, SO_x, NO_x, and NMHC from both mobile and stationary sources. This could explain the trend for $PM_{2.5}$ in Xiaogang and Daliao for the years 2005–2017. The variations in the $PM_{2.5}$ concentration in winter and summer can be explained by the north and south winds, which are dominant during winter and summer, respectively (Tsai *et al.*, 2003). During winter, the dominance of the north wind reduces the possibility of vertical diffusion of $PM_{2.5}$ in the mixed layer.

The $PM_{2.5}$ concentration in summer ranges from 13.7–18.0 μg m^{-3} as shown in Fig. 3. This is below the 24-hour standard in Taiwan. Water-soluble ions account for the largest proportion in the total $PM_{2.5}$ mass, with an average of 7.4 and 22.7 μg m^{-3} in summer and winter respectively of the total $PM_{2.5}$ mass. In summer, the carbon composition by mass exceeded the contribution from other chemicals in site C only. However, in winter, the concentration of other chemicals exceeded that of the carbon content in all sites. The average carbon content was 11.8% and 34.2% in summer and winter, respectively. The mass composition in winter exceeded that of summer because of lower wind recirculation, which limited dilution rates (Virtanen *et al.*, 2006; Tseng *et al.*, 2019). The average mass concentrations of EC and OC in the atmospheric $PM_{2.5}$ for the summer and winter seasons for the four sites under investigation are shown in Fig. 4. The seasonal average OC content ranged between 1.2 and 3.0 μg m^{-3} in summer while the range for winter is between 5.6 to 6.2 μg m^{-3}. The range of EC content was wider in the summer than in the winter. In summer, it ranged from 0.6 to 1.8 μg m^{-3} while in winter it ranged from 1.7 to 2.2 μg m^{-3}. EC is emitted from the incomplete combustion of fuels while OC results from the degradation of carbonaceous materials. The dominance of either EC or OC indicates the major source of carbonaceous aerosols.

Carbonaceous aerosols form a major component of PM and play an important role in atmospheric chemistry. Investigations carried out in the past found that the OC/EC in the region ranged between 2.32 and 2.76 in periods when the sea and land breeze interacted (Fang *et al.*, 2008). Herein, the OC/EC ratio ranged between 1.5 to 4.0. This indicates that the predominant sources of carbon content in $PM_{2.5}$ are photochemical reactions, industrial, and combustion processes. This is in line with previous studies on carbon compositions in $PM_{2.5}$ in the Kaohsiung

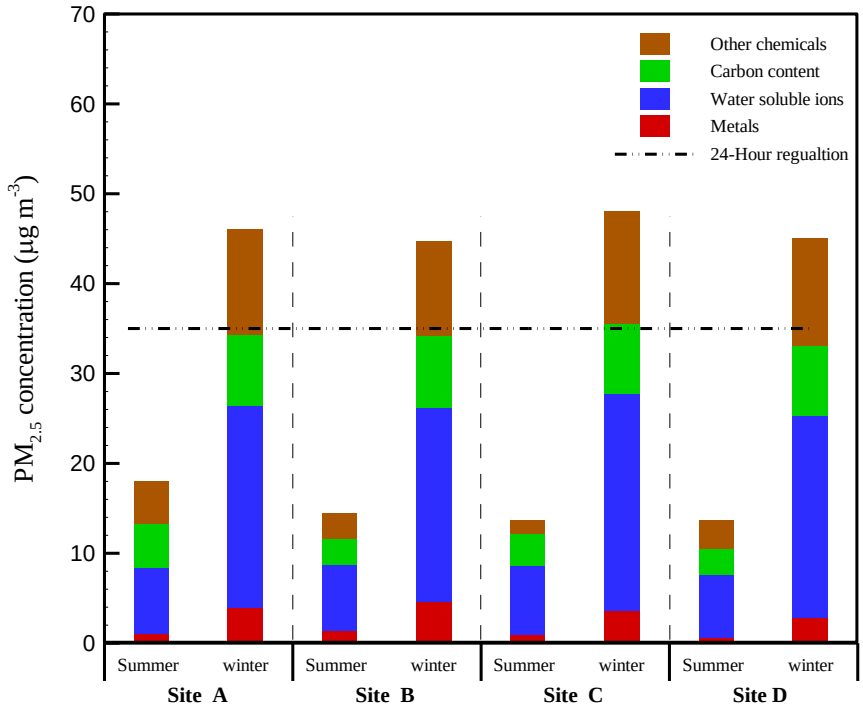

Fig. 3. The speciation of $PM_{2.5}$ during different seasons and at different sites of investigation.

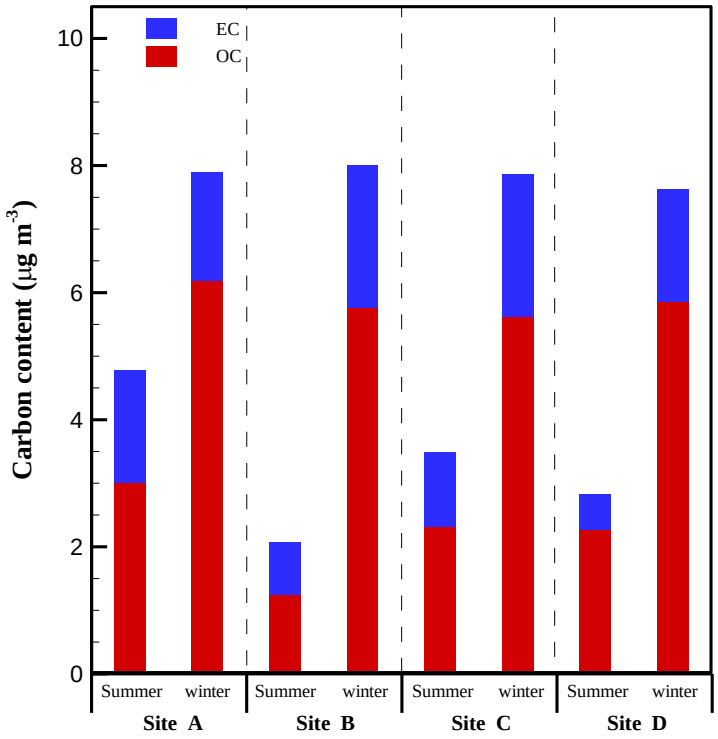

Fig. 4. Mass of elemental and organic carbon in $PM_{2.5}$ and the ratios of OC/EC for different sites during summer and winter.

metropolitan area. For instance, Huang (1991) found that carbon content accounted for about 22.1% of the ambient air $PM_{2.5}$, on average, and the average OC/EC ratio was 2.6. The OC/EC ratio can be applied to determine the intensity of secondary organic aerosol formation. The critical value is OC/EC =2.2 or OC/TC = 0.67. Carbon component analysis methods include thermal decomposition method (TM), solvent extraction (SEM), thermal manganese oxidation method (TMO), thermo-optical reflection method (TOR) optics, and thermo-optical transmission method (TOT). For sites A, B, and C, during summer the OC/EC value is less than 2.2 indicating a low potential for the formation of secondary organic aerosols (SOA). In summer, the OC/EC for Site D greatly exceeded that found at the other sites. This is because site D is a rural area, and therefore, the degradation of carbon-containing products such as vehicle tires and vegetation, leads to more carbonaceous aerosol emissions compared to that derived from incomplete combustion of carbon-containing fuels.

At other times, the OC/EC ratio in all sites during winter exceeded 2.2, indicating a high potential for the formation of SOA (Pandis *et al.*, 1992; Cao *et al.*, 2008). Overall, carbonaceous $PM_{2.5}$ are mainly emitted from combustion sources upwind of the site under investigation, including mobile sources and fixed sources, such as the petrochemical industry, boilers, steelmaking processes, and secondary derived aerosols.

3.2 Chemical Speciation of Ambient Air $PM_{2.5}$

The concentrations of $PM_{2.5}$ and their speciation at the sites under investigation for two seasons are presented in Fig. 3. The concentration during winter exceeded that of summer for all sites. Further, it can be observed that metals had the lowest concentrations in all sites and for all seasons. The most important category of chemicals is water-soluble ions. Site B has the highest metal composition while site D had the lowest concentration of metals and water-soluble ions. This phenomenon can be attributed to the proximity of the respective sites to the raw material storage site and the dominant wind directions (Cohen *et al.*, 2011).

3.3 Metal Composition

The profile for metals during summer is shown in Fig. 5(a), Site D had the highest concentrations

of Na and K. Al was lacking at all the sites except site A. Ca is the only metal of natural origin that was absent at all sites. Mn was present at site B only while Zn was present in all sites. Other metals of anthropogenic origin were absent at all the sites. During winter, all metals of natural origin were present at all sites except Al, which was absent at site A. Other than V, Mn, Zn, and Pb, other metals of anthropogenic origin were absent at all sites under investigation. The metallic elements in the $PM_{2.5}$ mostly exist in the solid phase and are distributed in the environment through atmospheric airflow or gravity sedimentation (Moreno *et al.*, 2004). During summer, the metal composition accounted for an average of 5.7% of the total mass of $PM_{2.5}$ at all the sites under investigation as shown in Fig. 3. Specifically, Na had the highest contribution, which were 35.2%, 25.1%, 45.9%, and 50.1% for sites A, B, C, and D, respectively.

The predominance of Na in summer can be attributed to the sea salt droplets occasionally blown by the westerly wind from the sea to the land surface. It is hypothesized that the main source of Fe is re-suspension from the iron ore piles in the raw material storage site. Besides, during steel production, ferromanganese (Fe-Mn), ferrosilicon (Fe-Si), and aluminium are added to remove excess oxygen. The background soil of surrounding areas is rich in crustal elements such as Si, K, Mn, and Mg. The northwest wind brings crustal elements and sea salt droplets. This

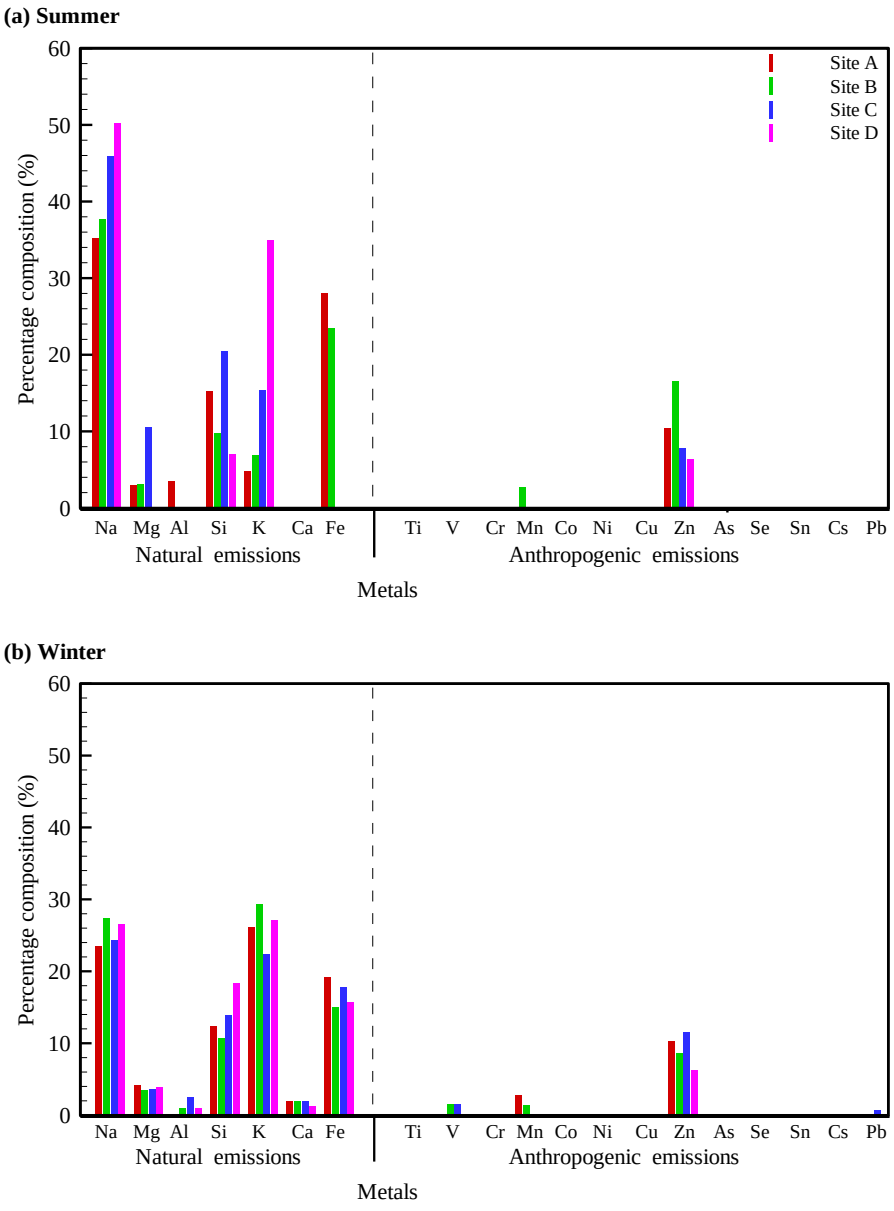

Fig. 5. $PM_{2.5}$ metal composition for sites A, B, C, and D during (a) summer (b) winter.

is believed to cause high concentrations of these crustal elements in $PM_{2.5}$. The proportion of Zn in the total mass of the metals ranged between 6.39% and 10.5%. The main source is believed to be the mobile sources in the sites under investigation (Lin *et al.*, 2020; Shen *et al.*, 2020).

3.4 Water-soluble Ions

In Fig. 6, the percentage composition of individual water-soluble ions is presented. During winter, SO_4^{2-} was the most important component at all the sites. In summer, NO_3^- was the most important composition. The percentage of SO_4^{2-} was almost constant for both seasons. In all seasons and for all sites, SO_4^{2-}, NO_3^-, and NH_4^+ contributed about 90% of the total water-soluble ions. The percentage composition of NH_4 in summer exceeded that of winter for all sites. In winter, the water-soluble ionic component, SO_4^{2-}, accounted for about 70% of the total water-soluble ions by mass, followed by NH_4^+ with an average of 10%, and NO_3^- with an average of 5%, ranking third, as shown in Fig. 3. The predominance of SO_4^{2-} and NO_3^- implies that anthropogenic sources have a higher contribution to ambient air $PM_{2.5}$ than natural sources. Information on the contribution of primary and secondary emission sources to ambient air $PM_{2.5}$ can be obtained from the ratios of SO_4^{2-} to NO_3^-. Further, as seen in Table 4, the percentage composition of SO_4^{2-} was significantly higher in pile 1 compared to the other piles. This can be used to paint a picture of the transformation phenomena of sulfate and nitrate ions (Colbeck and Harrison, 1984). Fine nitrate has been associated with aerosol acidity and moisture content. Additionally, the oxygen isotopic anomalies of SO_4^{2-} and NO_3^- in $PM_{2.5}$ are transferred to O_3 during the oxidation process of SO_2 an NO_x.

The I and J values for summer and winter for the four sites are presented in Fig. 7. For all sites, the I and J values exceeded the threshold during winter. On the other hand, they fell below the threshold during winter. The main constituents of secondary derived inorganic salts in the atmosphere NH_4^+, NO_3^- and SO_4^{2-}, easily exist in the air as NH_4NO_3, NH_4HSO_4, $(NH_4)_2SO_4$, and other types of salts. Previously, it was pointed out that is the equivalent concentration ratio of ammonium and sulfate (Seinfeld *et al.*, 1998). When the value of $I \geq 2$, it implies that SO_4^{2-} has been neutralized and mainly exists as $(NH_4)_2SO_4$. On the other hand, if $I < 2$ then only part of it exists as $(NH_4)_2SO_4$, and free sulfate ions still exist in the atmosphere.

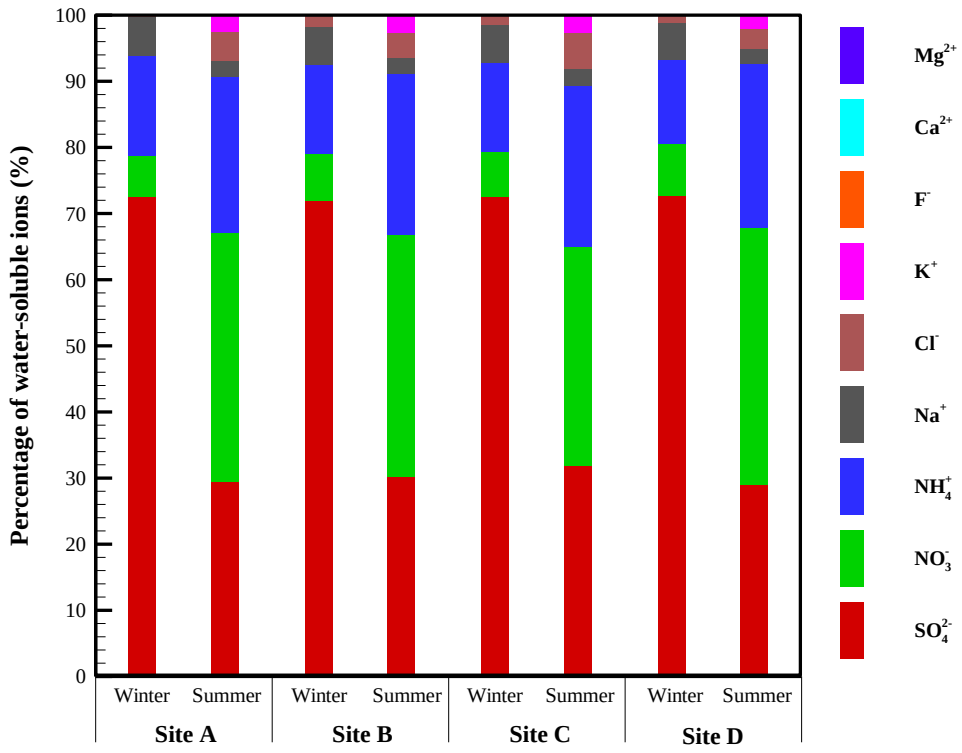

Fig. 6. Percentage of water-soluble ions in $PM_{2.5}$.for the seasons of winter and summer and at sites A, B, C, and D.

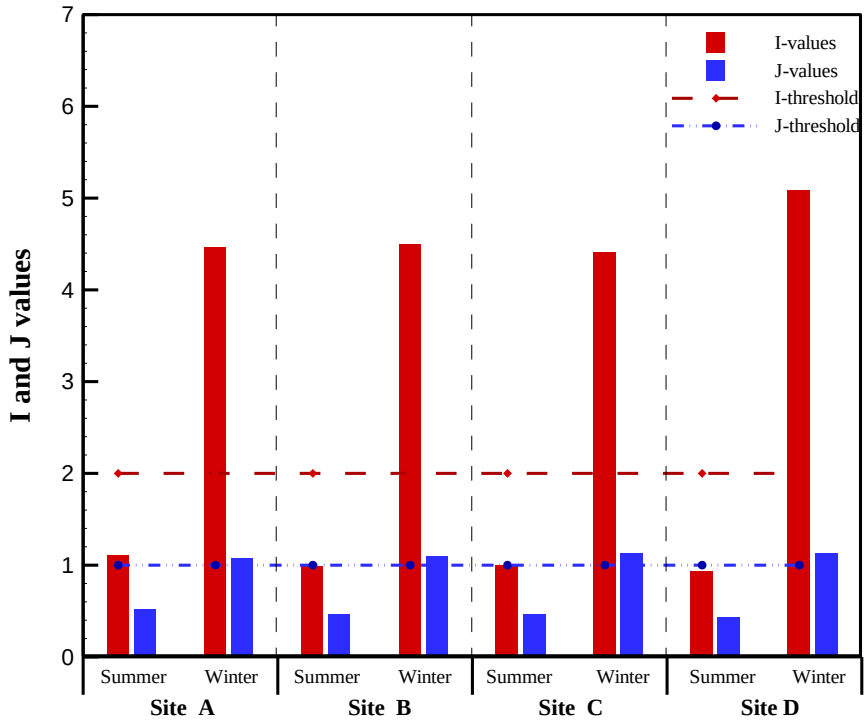

Fig. 7. I and J values for $PM_{2.5}$ and the thresholds in sites A, B, C, and D for summer and winter.

$$I = \frac{NH_{4\,eq}^{+}}{SO_{4\,eq}^{2-}} \tag{2}$$

The 24-hour ratio of NH_4^+ to NO_3^- and SO_4^{2-} ratio is represented by the J value (Chu, 2004). When $J < 1$, then NH_4^+ is insufficient to neutralize NO_3^- and SO_4^{2-} and therefore, they are acidic. On the other hand, if $J > 1$, NH_4^+ is in surplus, and NO_3^- and SO_4^{2-} are basic.

$$J = \frac{NH_{4\,eq}^{+}}{2 \times SO_{4\,eq}^{2-} + NO_{3\,eq}^{-}} \tag{3}$$

Herein, the value of I ranged between 0.81and 1.30 while the J value ranged between 0.37–0.60, $I < 2$, $J < 1$, indicating the presence of NO_3^- and SO_4^{2-} and an acidic atmosphere.

From Table 4, the percentage composition of SO_4^{2-} was significantly higher in pile 1 compared to the other piles. Further, water-soluble ions formed the most important component in the limestone piles especially, SO_4^2, Ca^{2+}. All these led to lower I and J ratios. While the percentage composition of SO_4^{2-} in the total $PM_{2.5}$ coal pile 1 exceeded 50%, that in the other coal piles barely reached 10%. This suggests that the contribution of coal piles to secondary aerosols was the highest in coal pile 1.

3.5 Carbon Content

From Fig. 4, the mass of organic carbon exceeded that of elemental carbon at all the sites under investigation and during all seasons. The OC/EC ratios for the four sites are presented in Table 3, where sites A and D had the highest values during summer. Carbon was a minor component in the iron ore pile, as shown in Table 4. Organic carbon exceeded elemental carbon in all piles except the third iron pile and this might indicate contamination. Unlike in the iron ore piles, carbon was the major component in the coal piles. The percentage composition of elemental carbon exceeded that of organic carbon in all piles except the second pile. The percentage composition of elemental carbon was more than 20% except in the first coal pile, where it was approximately 2%. The percentage composition of carbon in the coal pile 1 was

attributed to high sulfate concentrations. The high sulphate content is hypothesized to originate from leaching of overlying steel slags.

As shown in Table 4, the carbon content was the second most dominant composition in the limestone piles with OC more abundant than EC (Tseng *et al.*, 2019). Only three metal types were present in significant percentage compositions in the three stone piles including Mg, Ca, and Fe. The other metal compositions were either insignificant or non-existent. As seen in Table 4, EC formed a significant percentage composition of the sinter pile, at about 21%. The rest of the compositions comprised less than 5% of the percentage composition. In the coke pile, OC exceeded EC, unlike in the sinter pile. The carbon component accounted for 17.4% of the total

Table 3. The concentrations of OC and EC and the OC/EC.

	Site A		Site B		Site C		Site D	
	Summer	Winter	Summer	Winter	Summer	Winter	Summer	Winter
OC (μg m^{-3})	3.00	6.20	1.20	5.80	2.30	5.60	2.30	5.90
EC (μg m^{-3})	1.80	1.70	0.80	2.30	1.20	2.20	0.60	1.80
OC/EC	1.70	3.61	1.48	2.56	1.93	2.50	4.04	3.28

Table 4. Percentage masses of individual components in each pile of raw material.

	Raw materials														
	Iron piles					Coal piles					Limestone piles			Coke	Sinter
	IP1 (%)	IP2 (%)	IP3 (%)	IP4 (%)	IP5 (%)	CP1 (%)	CP2 (%)	CP3 (%)	CP4 (%)	CP5 (%)	LP1 (%)	LP2 (%)	LP3 (%)	pile (%)	pile (%)
Na	2.42	0.51	0.24	0.17	0.39	3.73	0.62	0.48	0.95	0.63	0.27	0.31	0.07	0.34	1.91
Mg	0.82	0.21	0.21	0.50	0.27	-	-	-	0.30	-	9.86	1.35	0.06	0.60	1.08
Al	7.54	0.46	1.39	2.07	2.06	2.03	0.64	1.09	1.24	0.95	0.30	0.46	0.09	0.89	2.16
Si	2.85	0.85	1.79	1.72	1.84	7.33	1.58	2.37	2.39	1.49	0.68	0.97	0.16	2.72	2.24
K	3.26	0.55	0.24	0.13	0.40	3.83	0.50	0.77	1.09	0.42	0.20	0.44	0.06	0.36	2.51
Ca	1.05	0.89	0.14	0.22	-	-	-	-	-	0.30	4.19	6.85	1.88	0.56	5.69
Ti	-	-	-	-	-	-	-	-	-	-	-	-	-	-	-
V	-	-	-	-	-	-	-	-	-	-	-	-	-	-	-
Cr	-	-	-	-	-	-	-	-	-	-	-	-	-	-	-
Mn	-	-	0.42	0.20	0.17	-	-	-	-	-	-	-	-	-	-
Fe	46.3	14.8	41.2	44.4	42.6	14.4	2.99	2.40	2.45	2.02	1.55	6.02	0.81	6.07	18.6
Co	-	-	-	-	-	-	-	-	-	-	-	-	-	-	-
Ni	-	-	-	-	-	-	-	-	-	-	-	-	-	-	-
Cu	-	-	-	-	-	-	-	-	-	-	-	-	-	-	-
Zn	-	-	-	-	-	-	-	-	-	0.50	-	-	-	-	0.19
As	-	-	-	-	-	-	-	-	-	-	-	-	-	-	-
Se	-	-	-	-	-	-	-	-	-	-	-	-	-	-	-
Sn	0.07	0.02	0.01	-	0.01	0.32	-	-	0.09	-	0.02	0.03	0.00	-	-
Cs	-	-	-	-	-	-	-	-	-	-	-	-	-	-	-
Pb	-	-	-	-	-	-	-	-	-	-	-	-	-	-	-
F^-	-	-	0.17	-	-	-	-	-	-	-	0.11	-	-	0.34	0.20
Cl^-	2.27	0.65	0.51	0.48	0.48	6.17	1.07	1.04	1.01	1.41	0.37	0.72	0.13	1.28	0.57
NO_3^-	1.27	0.23	0.34	0.27	0.31	2.68	0.59	0.70	0.80	0.59	0.17	0.31	0.06	0.51	0.34
SO_4^{2-}	22.7	5.83	4.63	4.19	6.59	55.3	10.8	11.1	9.62	11.4	3.86	4.93	39.5	11.41	5.85
Na^+	-	-	-	-	-	-	-	-	-	-	-	-	-	-	-
NH_4^+	-	-	-	-	-	-	-	-	-	-	-	-	-	-	-
K^+	-	-	-	-	-	-	-	-	-	-	-	-	-	6.58	-
Ca^{2+}	-	2.39	-	1.20	0.40	-	-	-	-	-	6.64	18.9	8.14	3.18	17.83
Mg^{2+}	-	-	-	-	-	-	-	-	-	-	2.54	-	-	-	-
OC	7.80	7.31	9.05	7.60	4.67	4.95	28.2	9.06	10.8	9.78	25.3	13.9	17.9	5.41	6.61
EC	2.40	0.95	11.3	0.00	0.08	1.50	20.1	25.4	39.8	41.9	10.6	1.73	2.24	22.0	2.73

Note: IP represents Iron piles; CP represents Coal piles; LP represents Limestone piles.

mass, where OC exceeded EC. The pollution source may have come from organic carbon derived from photochemical reactions or pollution emissions such as industrial combustion (Hays *et al.*, 2005).

3.6 Chemical Fingerprints for the $PM_{2.5}$ in the Raw Material Piles

The chemical profiles of different types of iron ore piles are presented in Table 4. As anticipated, Fe content in the iron pile ranged from 14.8 to 46.3% and hence was the most abundant species in all five iron piles. Coal pile 1 had a significant amount of Na, Al, Si, K, and Fe. The percentage composition of all metals was less than 10% in all five iron piles, except for Fe in core pile 1, which was 14.4%. The percentage composition of metals in the other piles was either non-existent or insignificant. Additionally, the iron piles had water-soluble ions and other crustal components. Among the water-soluble ions, SO_4^{2-} was present in the highest concentration. In Iron pile 1, it was 22% while in the other piles it ranged between 4 and 6%. Aluminium was present in the highest percentage in iron pile 1, while in the other piles, it was less than 2%. The crustal elements included Na, Mg, Al, K, and Si, while the water-soluble ions included four anionic species such as SO_4^{2-}, NO^-, Cl^-, F^-, and 5 cationic species including Na^+, K^+, Ca^{2+}, Mg^{2+}, NH_4^+. Among the water-soluble ions, SO_4^{2-} was the most abundant water-soluble ion accounting for (4.2–22%) in all piles. OC content was highest in Iron pile 1 at 11.3% while in the other iron piles, it ranged between 4.7–9.1%. This was suspected to contribute to the ambient air $PM_{2.5}$ through re-suspension especially during the sea-land breeze associated with periods with no precipitation in winter (Cao *et al.*, 2008).

The composition of coal pile 1 as presented in Table 4 differed from the other coal piles. Its main component was SO_4^{2-}, which contributed 55.3% of all water-soluble ions. The metal composition was 31.6% while that of carbon was 6.45%. The carbon content was high in the other four coal piles. In coal pile 2, organic carbon (28%) exceeded elemental carbon (20.1%) unlike in the other coal piles (Moreno *et al.*, 2004; Fang *et al.*, 2008). The elemental carbon ranged between 25.4–41.9% while the organic carbon ranged between 9.06–10.8%. Water-soluble ions accounted for between 11.4–12.0%, where SO_4^{2-} was responsible for 9.62–11.4%. The metal composition was 6.32–8.51%, and the contribution from crustal elements was insignificant. As shown in Table 4, Ca^{2+} and Fe comprised the highest percentage composition of the sinter pile, with about 20% each (Moreno *et al.*, 2004; Fernández-González *et al.*, 2017). One possible reason for the high Ca^{2+} was the contamination of the sinter pile with dust from the limestone pile, which naturally has high concentrations of Ca^{2+}. Additionally, within an integrated steel plant, the presence of oxygen species during reduction and refining processes causes the expulsion of low molecular weight metals in the form of fine particulates. Further, the leaching of steel slags for long periods could also explain the high Ca^{2+} concentration.

In the limestone pile, the three piles differed significantly in terms of chemical composition. In limestone pile 1, total carbon accounted for 35.9% while metals accounted for 17%. Specifically, elemental carbon was 10.6%, and organic carbon was 25.3 %. For the metal composition, magnesium and calcium accounted for 9.86% and 4.19% respectively. Water-soluble ions accounted for 13.2%, where the individual contributions from Ca^{2+}, SO_4^{2-}, and Mg^{2+} were 6.64%, 3.86%, and 2.54%, respectively. In limestone pile-2, water-soluble ions were the main chemical composition where Ca^{2+} and SO_4^{2-} accounted for 18.9% and 4.93% respectively. Metals and carbon accounted for 16.4% and 15.6% respectively. Specifically, organic carbon accounted for 13.9%. Stone pile 3 had water-soluble ions as the main components, just like stone pile 2. They accounted for 47.7% of the total chemical composition, with SO_4^{2-} accounting for 39.5%. Carbon accounted for 20.2%, and metals contributed 3.13%. As anticipated, Ca^{2+} was among the major components in limestone and could have contributed Ca^{2+} in the ambient air $PM_{2.5}$ after re-suspension (Monshi and Asgarani, 1999).

The main chemical component in the coke pile was carbon, which accounted for 27.4%. Water-soluble ions and metal accounted for 21.7% and 11.6%, respectively. Specifically, SO_4^{2-}, K^+, and Ca^{2+} contributed 11.4%, 6.58%, and 3.18% respectively whereas Fe, Si, and Al accounted for 6.07%, 4.19%, and 0.89%, respectively. In the case of the sinter pile, the metal component was the most important, accounting for 37.4%. Specifically, the contributions from Fe, Ca, K, Si, Al, Na, and Mg were 18.6%, 5.69, 2.51, 2.24, 2.16, 1.91, and 1.08%, respectively. $PM_{2.5}$ from the coal mine was less dense compared to the other raw material piles and hence had a wider range of diffusion. The $PM_{2.5}$ from limestone and iron ore were characterized by high density, which

resulted in smaller diffusion distances from the raw material piles to adjacent locations (Moreno *et al.*, 2004; Cohen *et al.*, 2011).

3.7 Contribution of Various Pollution Sources from the Receptor Model (CMB)

The results for the seasonal variations and fingerprint data for pollution sources are summarized in Table 5. Based on the compositional analysis, the main sources of $PM_{2.5}$ in the neighborhood of the raw material storage field were hypothesized to be petrochemical plants, boilers, background soil dust, secondary sources of sulfates and nitrates, and combustion sources. During winter, the main pollution sources of $PM_{2.5}$ for sites A, B, and C was the petrochemical industry where it accounted for 20.6%, 22.8%, and 17.8% of the total $PM_{2.5}$ mass, respectively. In site D, secondary nitrates accounted for the highest $PM_{2.5}$ mass at (19.3%. Secondary nitrates (NO_3^-) were mostly from mobile sources and other combustion sources upstream (Yang *et al.*, 2019). Ammonium released from fertilizers and animal feeds is also believed to have contributed to the high concentrations of nitrates and sulfates in $PM_{2.5}$ especially in site D. The petrochemical industry was dominant in sites A, B, and C because of their proximity to the petroleum product processing plant. In addition to nitrates and sulfates, the boiler and background soil were dominant ambient $PM_{2.5}$ sources in site D due to the dominating influence of the land-sea breeze and lack of rainfall (Lee *et al.*, 2008; Yuan *et al.*, 2018).

The average contributions of the major pollution sources during summer for site A included sulfate (28.70%), traffic sources (16.36%), and soil dust (13.38%). Those for site B included sulfate (43.47%) and traffic sources (13.74%). For site C, they were derived sulfate (36.95%), traffic sources (14.19%), and derived organic carbon (13.85%), and those for site D included sulfate (35.34%), soil dust (27.44%), and organic carbon (14.91%). Overall, secondary aerosols were the predominant form of $PM_{2.5}$ in the area under investigation. Site A was predominantly affected by the west and northwest winds. Therefore, the petrochemical plant located on the west side of the raw material storage site was an important source of $PM_{2.5}$. Through CMB, it was established that emissions from the petrochemical plant, boiler, and incinerator flow towards the raw material storage site led to an increase in the ambient air sulfate concentrations (Hu *et al.*, 2019). At site B, during the summer, the station is affected by the northwest west wind, and south wind, bringing sea droplets to the station. Site C was greatly influenced by sea salt droplets under the influence of sea and land breezes. Site D had no obvious pollution source during summer except mobile sources, which led to amplified nitrate composition in the $PM_{2.5}$. At site D, the crustal composition, as well as the contribution from mobile sources, were the predominant components of $PM_{2.5}$. Additionally, this site was adjacent to the petrochemical plant and therefore, under the influence of pollutants transported by the west, southwest, and northeast winds as well as the land-sea breezes (Cohen *et al.*, 2004; Fang *et al.*, 2018). The dominance of sulfates and secondary OC in summer for all sites indicates active biogenic sources in the neighborhood.

Table 5. Percentage contributions of $PM_{2.5}$ sources to the surrounding of the raw material storage site according to the chemical mass balance

		Pollution sources																			
		I (%)	II (%)	III (%)	IV (%)	V (%)	VI (%)	VII (%)	VIII (%)	IX (%)	X (%)	XI (%)	XII (%)	XIII (%)	XIV (%)	XV (%)	XVI (%)	XVII (%)	XVIII (%)	IXX (%)	XX (%)	Total (%)
Winter	Site A	3.2	0.0	0.0	0.0	20.6	0.0	0.0	6.7	5.8	4.2	0.0	0.0	0.0	2.3	2.2	12.4	18.5	0.0	0.9	23.3	100
	Site B	4.4	7.4	0.0	0.0	22.8	0.0	0.0	5.1	0.8	6.2	0.0	0.0	0.0	2.4	1.6	10.6	17.0	0.0	0.7	20.9	100
	Site C	1.5	2.8	2.8	0.0	17.8	0.0	0.9	4.9	2.5	3.2	0.0	0.0	0.0	3.2	3.6	13.9	17.4	0.0	0.0	25.6	100
	Site D	0.0	0.0	0.0	0.0	2.8	0.0	18.0	7.0	0.0	0.0	0.0	0.0	0.0	11.8	1.5	13.2	19.3	8.9	1.1	16.4	100
Summer	Site A	0.3	3.1	0.0	0.0	9.6	0.0	0.0	16.4	3.6	0.0	0.0	0.0	0.0	13.4	3.8	28.7	2.6	9.2	0.0	9.4	100
	Site B	0.0	0.0	0.0	0.0	3.4	0.0	0.0	13.7	3.6	4.1	0.0	0.0	0.0	1.2	4.9	43.5	5.0	8.6	0.0	12.1	100
	Site C	0.0	0.0	0.0	0.0	0.0	0.0	0.0	14.2	0.0	0.0	0.0	0.0	0.0	18.9	6.8	36.9	3.0	13.8	0.0	6.4	100
	Site D	0.0	0.0	0.0	0.0	0.0	0.0	0.0	6.5	0.0	0.0	0.0	0.0	0.0	27.4	4.7	35.3	3.6	14.9	0.0	7.5	100

Note: I-Steel plant's converter, II-Coke Furnace, III-Sinter Furnace, IV-Electric Arc Furnace, V-Petrochemical Industry, VI-Incinerator, VII- Boiler, VIII-Traffic source, IX-Iron ore, X-Coal ore, XI-Stone ore, XII-Coke ore, XIII-Sinter ore, XIV-Soil dust, XV-Marine aerosol, XVI-Secondary sulfate, XVII-Secondary nitrate, XVIII-Secondary OC, IXX-Secondary EC, XX-Others.

4 CONCLUSIONS

The main goal of these investigations was to establish the contribution of a raw material storage site to ambient air $PM_{2.5}$ in the surrounding area. The major chemical compositions of resuspended $PM_{2.5}$ from iron ore, coal, limestone, coke, and sinter piles were successfully investigated. The chemical composition differed among the various piles. Furthermore, there were slight variations among piles with the same key compositions. The variations in the concentration of $PM_{2.5}$ between the two seasons indicated that prevailing weather conditions, such as the dominant wind direction, temperature, and rainfall, significantly affected the $PM_{2.5}$ concentrations. Lower wind intensities in winter as compared to summer led to inadequate circulation of air masses and hence elevated concentrations of $PM_{2.5}$ within the site under investigation during winter. In the summer, the $PM_{2.5}$ concentration ranged from 13.7–18 μg m^{-3}, and water-soluble ions accounted for 54.2% of the total. The main ambient $PM_{2.5}$ components were SO_4^{2-} (73.6%), NH_4^+ (13.7%) and NO_3^- (7.45%). In winter, the $PM_{2.5}$ ranged between 44.7 and 48.0 μg m^{-3}, and water-soluble ions accounted for 49.2% of the $PM_{2.5}$ total mass. The main components were NO_3^- (36.5%), SO_4^{2-} (30.1%), and NH_4^+ (24.3%). In the winter, the relative humidity (above 70%) and the low-temperature environment led to high ambient air NO_3^- concentrations. The site selected for material storage has a more obvious impact on the regions downwind. The OC/EC ratios indicated that the predominant sources for ambient air $PM_{2.5}$ were photochemical, industrial, and combustion processes. However, the surroundings of the raw material storage site are affected more by other notable pollution sources, including petrochemical plants, soil dust, derived sulfates and nitrates, and mobile sources. The dominance of secondary organic aerosols raises concerns about the importance of dealing with the emission of secondary aerosol precursors.

REFERENCES

Ahmad, T., Park, J., Keel, S., Yun, J., Lee, U., Kim, Y., Lee, S.S. (2018). Behavior of heavy metals in air pollution control devices of 2,400 kg/h municipal solid waste incinerator. Korean J. Chem. Eng. 35, 1823–1828. https://doi.org/10.1007/s11814-018-0101-1

Artíñano, B., Salvador, P., Alonso, D.G., Querol, X., Alastuey, A. (2003). Anthropogenic and natural influence on the PM_{10} and $PM_{2.5}$ aerosol in Madrid (Spain). Analysis of high concentration episodes Environ. Pollut. 125, 453–465. https://doi.org/10.1016/S0269-7491(03)00078-2

Bell, M.L., Ebisu, K., Leaderer, B.P., Gent, J.F., Lee, H.J., Koutrakis, P., Wang, Y., Dominici, F., Peng, R.D. (2014). Associations of $PM_{2.5}$ constituents and sources with hospital admissions: Analysis of four counties in connecticut and Massachusetts (USA) for persons ≥ 65 years of age. Environ. Health Perspect. 122, 138–144. https://doi.org/10.1289/ehp.1306656

Benchrif, A., Guinot, B., Bounakhla, M., Cachier, H., Damnati, B., Baghdad, B. (2018). Aerosols in Northern Morocco: Input pathways and their chemical fingerprint. Atmos. Environ. 174, 140–147. https://doi.org/10.1016/j.atmosenv.2017.11.047

Cao, J.J., Chow, J.C., Watson, J.G., Wu, F., Han, Y.M., Jin, Z.D., Shen, Z.X., An, Z.S. (2008). Size-differentiated source profiles for fugitive dust in the Chinese Loess Plateau. Atmos. Environ. 42, 2261–2275. https://doi.org/10.1016/j.atmosenv.2007.12.041

Chalupa, D.C., Morrow, P.E., Oberdörster, G., Utell, M.J., Frampton, M.W. (2004). Ultrafine particle deposition in subjects with asthma. Environ. Health Perspect. 112: 879–882. https://doi.org/10.1289/ehp.6851

Chen, C.S., Chen, Y.L. (2003). The rainfall characteristics of Taiwan. Mon. Weather Rev. 131, 1323–1341. https://doi.org/10.1289/ehp.6851

Choi, L.T., Tu, J., Li, H., Thien, F. (2007). Flow and particle deposition patterns in a realistic human double bifurcation airway model. Inhalation Toxicol. 19, 117–131. https://doi.org/10.1080/08958370601051719

Chu, S.H. (2004). $PM_{2.5}$ episodes as observed in the speciation trends network. Atmos. Environ. 38, 5237–5246. https://doi.org/10.1016/j.atmosenv.2004.01.055

Cohen, D.D., Garton, D., Stelcer, E., Hawas, O., Wang, T., Poon, S., Kim, J., Choi, B.C., Oh, S.N., Shin, H.J., Ko, M.Y., Uematsu, M. (2004). Multielemental analysis and characterization of fine aerosols at several key ACE-Asia sites. J. Geophys. Res. 109, D19S12. https://doi.org/10.1029/2003JD003569

Cohen, D.D., Stelcer, E., Garton, D., Crawford, J. (2011). Fine particle characterisation, source apportionment and long-range dust transport into the Sydney Basin: A long term study between 1998 and 2009. Atmos. Pollut. Res. 2, 182–189. https://doi.org/10.5094/APR.2011.023

Colbeck, I., Harrison, R.M. (1984). Ozone—secondary aerosol—visibility relationships in North-West England. Sci. Total Environ. 34, 87–100. https://doi.org/10.1016/0048-9697(84)90043-3

Cullen, J.M., Allwood, J.M., Bambach, M.D. (2012). Mapping the global flow of steel: from steelmaking to end-use goods. Environ. Sci. Technol. 46, 13048–13055. https://doi.org/10.1021/es302433p

de la Campa, A.M.S., de la Rosa, J.D., Gonzalez-Castanedo, Y., Fernandez-Camacho, R., Alastuey, A., Querol, X., Pio, C. (2010). High concentrations of heavy metals in PM from ceramic factories of Southern Spain. Atmos. Res. 96, 633–644. https://doi.org/10.1016/j.atmosres.2010.02.011

Dejmek, J., Selevan, S.G., Benes, I., Solanský, I., Srám, R.J. (1999). Fetal growth and maternal exposure to particulate matter during pregnancy. Environ. Health Perspect. 107, 475–480. https://doi.org/10.1289/ehp.99107475

Fang, G.C., Wu, Y.S., Chou, T.Y., Lee, C.Z. (2008). Organic carbon and elemental carbon in Asia: A review from 1996 to 2006. J. Hazard. Mater. 150, 231–237. https://doi.org/10.1016/j.jhazmat.2007.09.036

Fang, J., Fan, J.M., Lin, Q., Wang, Y.Y., He, X., Shen, X.D., Chen, D.L. (2018). Characteristics of airborne lead in Hangzhou, southeast China: Concentrations, species, and source contributions based on Pb isotope ratios and synchrotron X-ray fluorescence based factor analysis. Atmos. Pollut. Res. 9: 607–616. https://doi.org/10.1016/j.apr.2017.12.009

Feng, J., Yu, H., Liu, S., Su, X., Li, Y., Pan, Y., Sun, J. (2016). $PM_{2.5}$ levels, chemical composition and health risk assessment in Xinxiang, a seriously air-polluted city in North China. Environ. Geochem. Health 39, 1071–1083. https://doi.org/10.1007/s10653-016-9874-5

Fernández-González, D., Ruiz-Bustinza, I., Mochón, J., González-Gasca, C., Verdeja, L.F. (2017). Iron ore sintering: Process. Miner. Process. Extr. Metall. Rev. 38, 215–227. https://doi.org/10.1080/08827508.2017.1288115

Hays, M.D., Fine, P.M., Geron, C.D., Kleeman, M.J., Gullett, B.K. (2005). Open burning of agricultural biomass: Physical and chemical properties of particle-phase emissions. Atmos. Environ. 39, 6747–6764. https://doi.org/10.1016/j.atmosenv.2005.07.072

Houck, J.E. (1991). Source sampling for receptor modeling, in: Hopke, P.K. (Ed.), Receptor Modeling for Air Quality Management, Elsevier Amsterdam, pp. 57–65. https://www.elsevier.com/books/receptor-modeling-for-air-quality-management/hopke/978-0-444-88218-9

Hu, J., Wang, H., Zhang, J., Zhang, M., Zhang, H., Wang, S., Chai, F. (2019). $PM_{2.5}$ pollution in Xingtai, China: Chemical characteristics, source apportionment, and emission control measures. Atmosphere 10, 121. https://doi.org/10.3390/atmos10030121

Lai, I.C., Brimblecombe, P. (2021). Long-range transport of air pollutants to Taiwan during the COVID-19 lockdown in Hubei province. Aerosol Air Qual. Res. 21, 200392. https://doi.org/10.4209/aaqr.2020.07.0392

Lee, S.W., Herage, T., He, I., Young, B. (2008). Particulate characteristics data for the management of $PM_{2.5}$ emissions from stationary combustion sources. Powder Technol. 180, 145–150. https://doi.org/10.1016/j.powtec.2007.03.025

Lin, C.H., Wu, Y.L., Lai, C.H., Watson, J.G., Chow, J.C. (2008). Air quality measurements from the southern particulate matter supersite in Taiwan. Aerosol Air Qual. Res. 8, 233–264. https://doi.org/10.4209/aaqr.2008.04.0012

Lin, Y.C., Li, Y.C., Amesho, K.T.T., Chou, F.C., Cheng, P.C. (2020). Filterable $PM_{2.5}$, metallic elements, and organic carbon emissions from the exhausts of diesel vehicles. Aerosol Air Qual. Res. 20, 1319–1328. https://doi.org/10.4209/aaqr.2020.02.0081

Loo, B.W., Jaklevic, J.M., Goulding, F.S. (1976). Dichotomous virtual impactors for large scale monitoring of airborne particulate matter. in: Liu, B.Y.H. (Ed.), Fine particles, Academic Press, pp. 311–350. https://doi.org/10.1016/B978-0-12-452950-2.50020-8

Monshi, A., Asgarani, M.K. (1999). Producing Portland cement from iron and steel slags and limestone. Cem. Concr. Res. 29, 1373–1377. https://doi.org/10.1016/S0008-8846(99)00028-9

Moreno, T., Merolla, L., Gibbons, W., Greenwell, L., Jones, T., Richards, R. (2004). Variations in the source, metal content and bioreactivity of technogenic aerosols: A case study from Port Talbot, Wales, UK. Sci. Total Environ. 333, 59–73. https://doi.org/10.1016/j.scitotenv.2004.04.019

Nogueira, J.B. (2009). Air pollution and cardiovascular disease. Rev. Port. Cardiol. 28, 715–733.

Pace, T.G. (1991). Receptor modeling in the context of ambient air quality standard for particulate matter, in: Hopke, P.K. (Ed.), Receptor modeling for air quality management, Elsevier Amsterdam, pp. 255–297. https://www.elsevier.com/books/receptor-modeling-for-air-quality-management/hopke/978-0-444-88218-9

Pandis, S.N., Harley, R.A., Cass, G.R., Seinfeld, J.H. (1992). Secondary organic aerosol formation and transport. Atmos. Environ. 26, 2269–2282. https://doi.org/10.1016/0960-1686(92)90358-R

Pöschl, U. (2005). Atmospheric aerosols: Composition, transformation, climate and health effects. Angew. Chem. Int. Ed. 44, 7520–7540. https://doi.org/10.1002/anie.200501122

Seinfeld, J.H., Pandis, S.N., Noone, K. (1998). Atmospheric chemistry and physics: From air pollution to climate change. Phys. Today 51, 88. https://doi.org/10.1063/1.882420

She, H., Cheng, P.H., Yuan, C.S., Yang, Z.M., Ie, I.R. (2020). Chemical characteristics, spatiotemporal distribution, and source apportionment of $PM_{2.5}$ surrounding industrial complexes in southern Kaohsiung. Aerosol Air Qual. Res. 20, 557–575. https://doi.org/10.4209/aaqr.2020.01.0007

Shen, H.Z., Yang, T.M., Lu, C.C., Yuan, C.S., Hung, C.H., Lin, C.T., Lee, C.W., Ling, G.H., Hu, G.R., Lo, K.C. (2020). Chemical fingerprint and source apportionment of $M_{2.5}$ in highly polluted events of southern Taiwan. Environ. Sci. Pollut. Res. 27, 6918–6935. https://doi.org/10.1007/s11356-019-07328-8

Tsai, S.S., Goggins, W.B., Chiu, H.F., Yang, C.Y. (2003). Evidence for an association between air pollution and daily stroke admissions in Kaohsiung, Taiwan. Stroke 34, 2612–2616. https://doi.org/10.1161/01.STR.0000095564.33543.64

Tseng, Y.L., Yuan, C.S., Bagtasa, G., Chuang, H.L., Li, T.C. (2019). Inter-correlation of chemical compositions, transport routes, and source apportionment results of atmospheric $PM_{2.5}$ in southern Taiwan and the northern Philippines. Aerosol Air Qual. Res. 19, 2645–2661. https://doi.org/10.4209/aaqr.2019.10.0526

Virtanen, A., Rönkkö, T., Kannosto, J., Ristimäki, J., Mäkelä, J., Keskinen, J., Pakkanen, T., Hillamo, R., Pirjola, L., Hämeri, K. (2006). Winter and summer time size distributions and densities of traffic-related aerosol particles at a busy highway in Helsinki. Atmos. Chem. Phys. 6, 2411–2421. https://doi.org/10.5194/acp-6-2411-2006

Wang, Y.S., Chang, L.C., Chang, F.J. (2020). Explore regional $PM_{2.5}$ features and compositions causing health effects in Taiwan. Environ. Manage. https://doi.org/10.1007/s00267-020-01391-5

Weijers, E., Schaap, M., Nguyen, L., Matthijsen, J., Van Der Gon, H.D., Ten Brink, H., Hoogerbrugge, R. (2011). Anthropogenic and natural constituents in particulate matter in the Netherlands. Atmos. Chem. Phys. 11, 2281–2294. https://doi.org/10.5194/acp-11-2281-2011

Wienke, D., Gao, N., Hopke, P.K. (1994). Multiple site receptor modeling with a minimal spanning tree combined with a neural network. Environ. Sci. Technol. 28, 1023–1030. https://doi.org/10.1021/es00055a010

Yang, H.H., Dhital, N.B., Wang, L.C., Hsieh, Y.S., Lee, K.T., Hsu, Y.T., Huang, S.C. (2019). Chemical characterization of fine particulate matter in gasoline and diesel vehicle exhaust. Aerosol Air Qual. Res. 19, 1439–1449. https://doi.org/10.4209/aaqr.2019.04.0191

Yuan, C.S., Lu, C.C., Shen, H.Z., Li, T.C. (2018). Metallic characteristics of $PM_{2.5}$ and $PM_{2.5\text{-}10}$ for clustered Aeolian Dust Episodes occurred in an extensive fluvial basin during rainy season. J. Air Waste Manage. Assoc. 68, 1085–1102. https://doi.org/10.1080/10962247.2018.1469554

Zhang, L., Wang, F., Ji, Y., Jiao, J., Zou, D., Liu, L., Shan, C., Bai, Z., Sun, Z. (2014). Phthalate esters (PAEs) in indoor PM_{10}/$PM_{2.5}$ and human exposure to PAEs via inhalation of indoor air in Tianjin, China. Atmos. Environ. 85, 139–146. https://doi.org/10.1016/j.atmosenv.2013.11.068

Zhao, J., Gao, Z., Tian, Z., Xie, Y., Xin, F., Jiang, R., Kan, H., Song, W. (2013). The biological effects of individual-level $PM_{2.5}$ exposure on systemic immunity and inflammatory response in traffic policemen. Occup. Environ. Med. 70, 426–431. https://doi.org/10.1136/oemed-2012-100864

Zhao, Y., Cui, K., Chen, S., Yin, Z., Chao, H.R., Chang-Chien, G.P. (2018). Atmospheric $PM_{2.5}$, total PCDD/Fs-WHO_{2005}-TEQ level and wet deposition: Cases of Jinan and Weihai cities, China. Aerosol Air Qual. Res. 18, 3081–3095. https://doi.org/10.4209/aaqr.2018.11.0395